Cell Cycle 13:3, 440–452; February 1, 2014; © 2014 Landes Bioscience

Mitotic phosphorylation of histone H3 threonine 80

Sharra L Hammond[1,2], Stephanie D Byrum[3], Sarita Namjoshi[1], Hillary K Graves[1], Briana K Dennehey[1] Alan J Tackett[3], and Jessica K Tyler[1,2,*]

[1]Department of Biochemistry and Molecular Biology; University of Texas; MD Anderson Cancer Center; Houston, TX USA; [2]Department of Molecular and Cellular Biology; Baylor College of Medicine; Houston, TX USA; [3]Department of Biochemistry and Molecular Biology; University of Arkansas for Medical Sciences; Little Rock, AR USA

Keywords: histone phosphorylation, mitosis, chromatin condensation

The onset and regulation of mitosis is dependent on phosphorylation of a wide array of proteins. Among the proteins that are phosphorylated during mitosis is histone H3, which is heavily phosphorylated on its N-terminal tail. In addition, large-scale mass spectrometry screens have revealed that histone H3 phosphorylation can occur at multiple sites within its globular domain, yet detailed analyses of the functions of these phosphorylations are lacking. Here, we explore one such histone H3 phosphorylation site, threonine 80 (H3T80), which is located on the nucleosome surface. Phosphorylated H3T80 (H3T80ph) is enriched in metazoan cells undergoing mitosis. Unlike H3S10 and H3S28, H3T80 is not phosphorylated by the Aurora B kinase. Further, mutations of T80 to either glutamic acid, a phosphomimetic, or to alanine, an unmodifiable residue, result in an increase in cells in prophase and an increase in anaphase/telophase bridges, respectively. SILAC-coupled mass spectrometry shows that phosphorylated H3T80 (H3T80ph) preferentially interacts with histones H2A and H4 relative to non-phosphorylated H3T80, and this result is supported by increased binding of H3T80ph to histone octamers in vitro. These findings support a model where H3T80ph, protruding from the nucleosome surface, promotes interactions between adjacent nucleosomes to promote chromatin compaction during mitosis in metazoan cells.

Introduction

The nucleosome is the basic repeating unit of DNA packaging in eukaryotes. It is composed of 2 of each of the 4 core histones, H2A, H2B, H3, and H4, around the outside of which is wound approximately 146 base pairs of DNA.[1] The nuclear genome is packaged into regular arrays of nucleosomes, which are further compacted by higher-order folding. Chromatin is compacted even more tightly during mitosis to facilitate chromosome segregation without breaking the DNA. However, the mechanisms by which mitotic chromatin compaction occurs are not clear, but appear to involve histone modification.

Histones are heavily modified by a wide range of post-translational modifications (PTMs), including phosphorylation, methylation, acetylation, and ubiquitylation. These modifications form a decipherable code, the "histone code", which is written by histone modifying enzymes, or "writers", and understood by effector proteins, or "readers".[2] Translation of this code plays an essential role in multiple cellular processes, including transcriptional regulation, DNA replication, DNA repair, and cell cycle progression. The vast majority of histone modifications occur on the N-terminal tails of histones. Those that are located on the histone globular domains are most abundant at the DNA–histone interface, where they appear to help regulate DNA–histone interactions.[3]

Of the 4 core histones, H3 is the most heavily modified. H3 has several phosphorylation sites, including threonine 3 (H3T3),[4] serine 10 (H3S10),[5] threonine 11 (H3T11),[6] serine 28 (H3S28),[7] threonine 45 (H3T45),[8] threonine 80 (H3T80),[9-12] and threonine 118 (H3T118).[13] Of these residues, the first 4 are located within the H3 N-terminal tail, and have been characterized previously. Both H3S10 and H3S28 are phosphorylated during mitosis by Aurora B kinase,[14-16] which is recruited to the centromeres upon phosphorylation of H3T3.[17] H3S10ph frequently occurs in the presence of methylation of the adjacent lysine residue, lysine 9 (H3K9). Here, the phosphorylation of H3S10 serves as a mechanism to disrupt the binding of the H3K9 methyl-binding protein HP1.[18,19] The timing of phosphorylation of H3S10 and H3S28 correlates with mitotic chromatin condensation, which begins in late G_2.[5,7] In *Tetrahymena,* phosphorylation of H3S10 is essential for both proper chromosome condensation and segregation.[20] However, in mammals, H3S10 is dispensable for both of these functions.[21,22] This leaves open the possibility that another histone modification at a different site may be important for chromosome condensation in metazoans.

Unlike the N-terminal phosphorylation sites, phosphorylation sites within the globular domain of H3 are poorly characterized. These sites include H3T45, H3T80, and H3T118. Unlike H3T45 and H3T118, which are located at the DNA–histone

*Correspondence to: Jessica K Tyler; Email: jtyler@mdanderson.org
Submitted: 10/18/2013; Accepted: 11/19/2013
http://dx.doi.org/10.4161/cc.27269

interface, H3T80 projects from the surface of the nucleosome. This position of H3T80ph makes it less likely to influence DNA–histone interactions, but more likely to be accessible to one or more reader proteins. Similar to H3S10 and H3S28, H3T80 is located adjacent to a lysine residue (H3K79), that is known to be mono-, di-, and tri-methylated.[23-25] Despite the identification of H3T80 phosphorylation (H3T80ph) in mammalian cells in 4 mass spectrometry studies, it has never been observed in the presence of H3K79 methylation (H3K79me).[9-12] Nonetheless, Martinez et al. used a commercial H3K79me3T80ph antibody to study histone H3K79me3T80ph in vivo.[26] However, our data shows that the H3K79me3T80ph antibody used previously actually recognizes H3K9me3S10ph, calling into question not only the existence of the H3K79me3H3T80ph dual modification, but also its dependence on the Aurora B kinase, and the proposed link between this dual modification and cancer. Furthermore, it highlights that H3T80ph, shown to exist via mass spectrometry studies, has not yet been characterized in vivo. Here we demonstrate, using an antibody specific to H3T80ph, that it is enriched during mitosis, but unlike other mitotic H3 phsophorylation marks such as H3S10ph and H3S28ph,[14-16] H3T80ph is not dependent on the Aurora B kinase and does not initiate at pericentric heterochromatin. Furthermore, mutations to prevent or mimic H3T80 phosphorylation result in mitotic defects. Functionally, phosphorylated H3T80 binds to other core histones leading us to propose that H3T80ph may promote chromatin condensation during mitosis.

Results

A commercially available H3K79me3T80ph antibody recognizes H3K9me3S10ph

Like most histone H3 residues, both H3T80 and the adjacent H3K79 are highly conserved (**Fig. 1A**). Spatially, H3T80 and H3K79 are located on the nucleosome surface with H3T80 positioned in such a way that it protrudes from the surface (**Fig. 1B**).[1] Previous work using a commercially available antibody raised against a H3K79me3T80ph peptide concluded that H3K79me3T80ph serves as a mitotic indicator in melanoma samples.[26] However, the staining pattern yielded by this antibody within the cell and the ablation of this signal by inhibitors of Aurora B kinase suggested to us the possibility that this putative H3K79me3T80ph antibody might recognize the highly abundant dual modification H3K9me3S10ph.[5,14-16] Therefore, we tested the specificity of this antibody (MC491) in 3 ways: dot blots with modified and unmodified H3 peptides; immunoblot analyses using lysates from cells lacking the H3K79 methyltransferase Dot1L;[27] and indirect immunofluorescence in cells reduced in their capacity to phosphorylate H3S10. On dot blots, and consistent with earlier work,[26] the MC491 antibody did not recognize H3S10ph alone. However, when the dual H3K9me3S10ph peptide was used, the MC491 antibody recognized both H3K9me3S10ph and H3K79me3T80ph peptides to similar extents (**Fig. 1C**). Immunoblot analyses revealed that the MC491 antibody recognized epitopes in both wild-type chicken DT40 cells and those lacking Dot1L, showing that it does not require methylation of H3K79 for epitope recognition (**Fig. 1D**). Likewise, indirect immunofluorescence analyses of HeLa cells treated with Hesperadin, an inhibitor of the Aurora B kinase that phosphorylates H3S10, resulted in a nearly complete loss of the MC491 antibody signal at concentrations that led to a pronounced reduction of H3S10ph signal (**Fig. 1E**). These data show that the MC491 antibody lacks specificity for H3K79me3T80ph in vitro and recognizes an epitope that is indistinguishable from H3K9me3S10ph in vivo. We also tested the specificity of a polyclonal H3K79me3T80ph antibody (Millipore 07–528) and found that it too recognized H3K9me3S10ph (data not shown). Given that there is no evidence for the coexistence of H3K79me3 and H3T80ph in vivo, we propose that the previous results obtained with this antibody[26] were all due to its recognition of the abundant dual modification H3K9me3S10ph in cells.

Generation of an antibody specific for H3T80ph

To discover for the first time the cellular localization of H3T80ph, we raised a rabbit monoclonal antibody against H3T80ph. Peptide dot blot analyses showed that multiple independent monoclonal antibodies recognized H3T80ph, but not other H3 phospho-residues, including H3S10ph. Furthermore, these antibodies recognized H3T80ph independent of the methylation state of the adjacent lysine residue (**Fig. 2A** and data not shown). The H3T80ph antibodies do not recognize any proteins, including H3, in western blots, indicating that they may only recognize the epitope containing H3T80ph when it is in a native conformation. To test whether or not the H3T80ph antibodies recognized full-length native H3, they were used for immunoprecipitation experiments. The H3T80ph antibodies immunoprecipitated histone H3 from cells that had been arrested at prometaphase with colcemid,[28] but not detectably from asynchronous cells (**Fig. 2B** and data not shown). This demonstrated that the H3T80ph antibodies recognized the native H3 protein and that H3T80ph may be a mitotically enriched histone modification. To confirm that the H3T80ph antibody specifically recognized native H3T80ph in cells, we performed indirect immunofluorescence-based peptide competition assays in HeLa cells. H3T80ph staining was competed away by an H3T80ph peptide, but not by the other phospho-H3 peptides including H3S10ph and H3K9me3S10ph (**Fig. 2C**). Finally, in contrast to the MC491 and H3S10ph antibodies (**Fig. 1D**), anti-H3T80ph signal was retained following Aurora B kinase inhibition with Hesperadin (**Fig. 2D**), even at concentrations that almost completely prevent H3S10ph detection. These experiments demonstrate that the H3T80ph antibody is specific for H3T80ph, and that the kinase that phosphorylates H3T80 is not the Aurora B kinase.

H3T80ph is enriched in mitosis in metazoan cells

Given that the H3T80ph antibody only precipitated H3 from cells arrested in mitosis (**Fig. 2B**), we wanted to further analyze the abundance of H3T80ph throughout the cell cycle. Flow cytometry analysis of HeLa cells showed that less than 4% of cells had H3T80ph signal above background levels, and these positive cells all had a 4N DNA content (**Fig. 3A**). This finding is not limited to HeLa cells nor cancer cell lines, as HCT-116, MCF7 (cancer cell lines), and MCF10A (non-cancer cell

line) cells all displayed a similar enrichment of H3T80ph in cells with a 4N DNA content (**Fig. 3B**). However, not all cells with a 4N DNA content were positive for H3T80ph, indicating that H3T80ph is unlikely to be enriched through all stages of G_2/M. Consequently, the precise spatial–temporal localization of H3T80ph during mitosis was examined via indirect immunofluorescence analysis in HeLa cells. H3T80ph was not detectable during interphase and became visible on chromatin in prophase. H3T80ph was maintained on the chromatin from prophase through metaphase, apparently being distributed throughout all regions of the chromosomes, but was no longer detectable in anaphase (**Fig. 3C**). In addition to the chromosomal staining of H3T80ph, H3T80ph is also apparent in the centrosomes during mitosis (see discussion). Taken together, these data show that H3T80ph is present on chromatin from prophase to metaphase of mitosis.

Histone H3 and the region around H3T80 are highly conserved (**Fig. 1A**), leading us to examine whether H3T80ph was also conserved in other eukaryotes. We were unable to detect any H3T80ph in either budding yeast or fission yeast by immunofluorescence (data not shown). However, H3T80ph was clearly present on the metaphase chromosomes of *Drosophila* S2 cells (**Fig. 4A**) and from prophase to early anaphase in mouse MM3MG cells (**Fig. 4B and C**). In the MM3MG cells, the H3T80ph levels were reduced by early anaphase and undetectable by late anaphase (**Fig. 4C**). Notably, H3T80ph foci were observed in MM3MG cells in the very early stages of mitosis that had already acquired H3S10ph (**Fig. 4C**). H3S10ph foci are known to initiate at the centromere before spreading throughout chromatin.[5] To determine whether or not H3T80ph foci were also present at the centromeres, cells

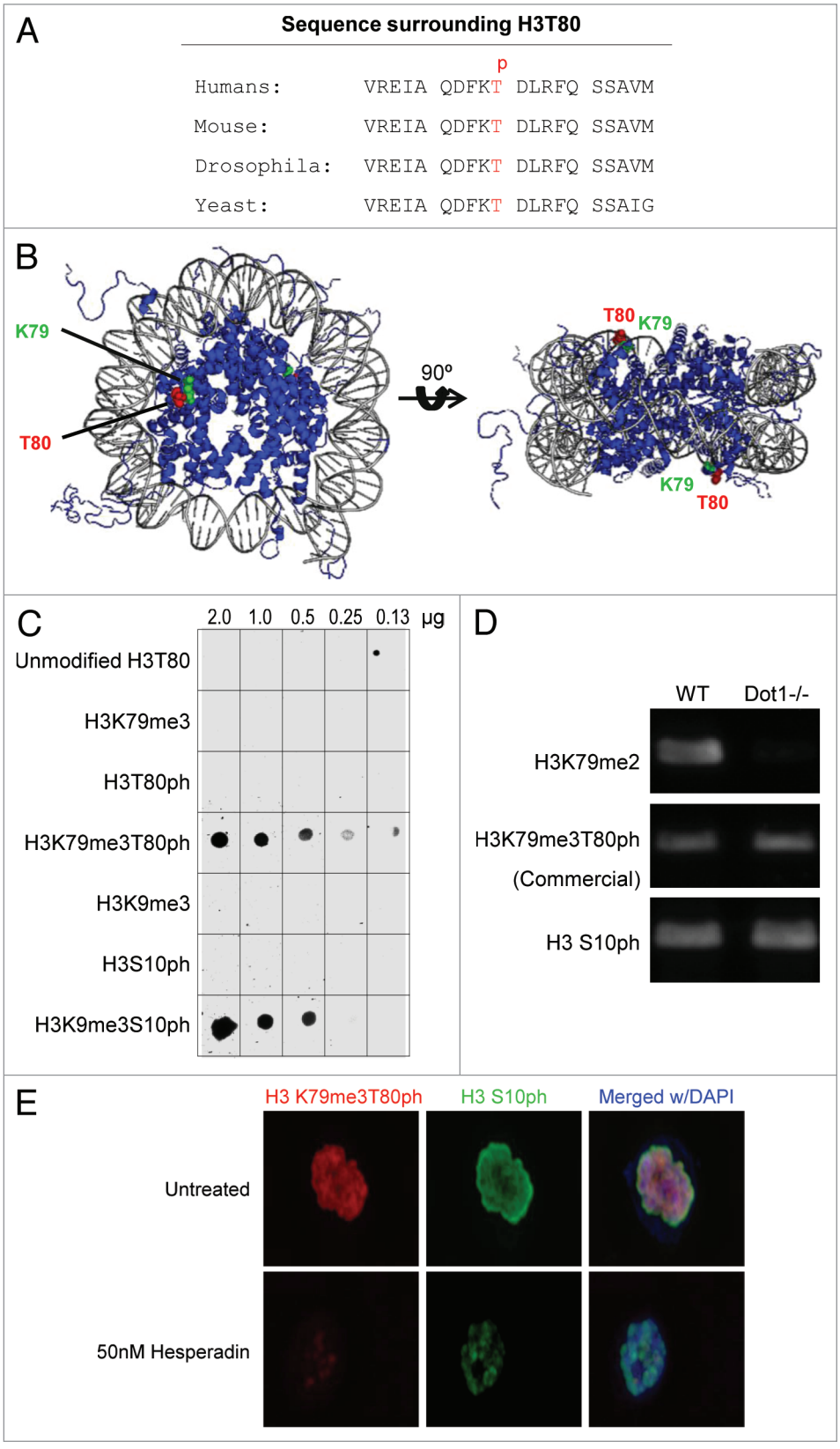

Figure 1. The commercial MC491 H3K79me3T80ph antibody recognizes H3K9me3S10ph. (**A**) Table showing the sequence identity surrounding the H3T80 residue. (**B**) Crystal structure of the nucleosome core.[27] H3T80 is indicated in red and H3K79 is indicated in green. (**C**) Dot blot analysis of MC491 using decreasing quantities of the indicated peptides. (**D**) Western blot analysis of MC491 using wild-type DT40 cells and Dot1L$^{-/-}$ DT40 cells.[28] H3K79me2 and H3S10ph were used as controls. (**E**) MC491 and H3S10ph staining of HeLa cells with or without Hesperidin treatment.

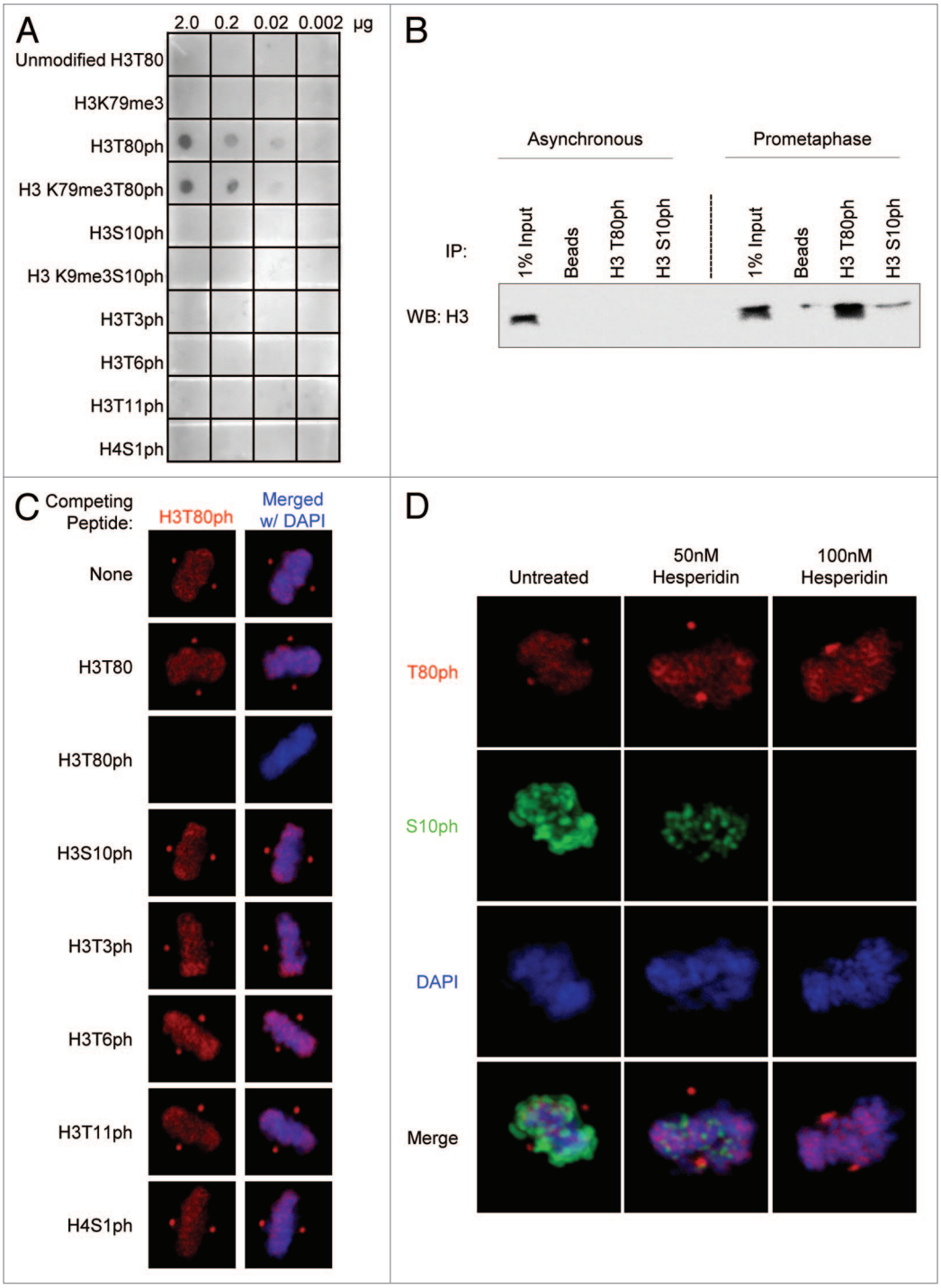

Figure 2. A new Histone H3T80ph antibody is specific. (**A**) Serially diluted peptides were dotted on PVDF membrane and probed with anti-H3T80ph. The antibody detects H3T80ph regardless of whether or not the adjacent lysine 79 is methylated. (**B**) Immunoprecipitation of H3 with H3T80ph antibody from prometaphase-arrested or asynchronous HeLa cells, probed with an anti-histone H3 antibody. (**C**) Peptide completion assays using the H3T80ph antibody competed against the indicated peptides. Antibody–peptide complexes were removed by centrifugation, and the remaining supernatant was used for immunofluorescence of formaldehyde-fixed HeLa cells. Shown are metaphase cells. (**D**) H3T80ph and H3S10ph staining of HeLa cells treated with 0–100 nM of Hesperidin.

were examined for the coincidence of H3T80ph and H3S10ph foci. H3T80ph foci did not co-localize with the most intense H3S10ph staining at the centromeres (**Fig. 4C**, first column), indicating that H3T80ph foci are not reflecting centromeric localization. The identity of the chromosomal localization of the H3T80ph foci in late G_2/early mitosis is not known, but this data indicates that H3T80ph does not initiate at pericentric heterochromatin, as is the case for H3S10ph and H3S28ph. This

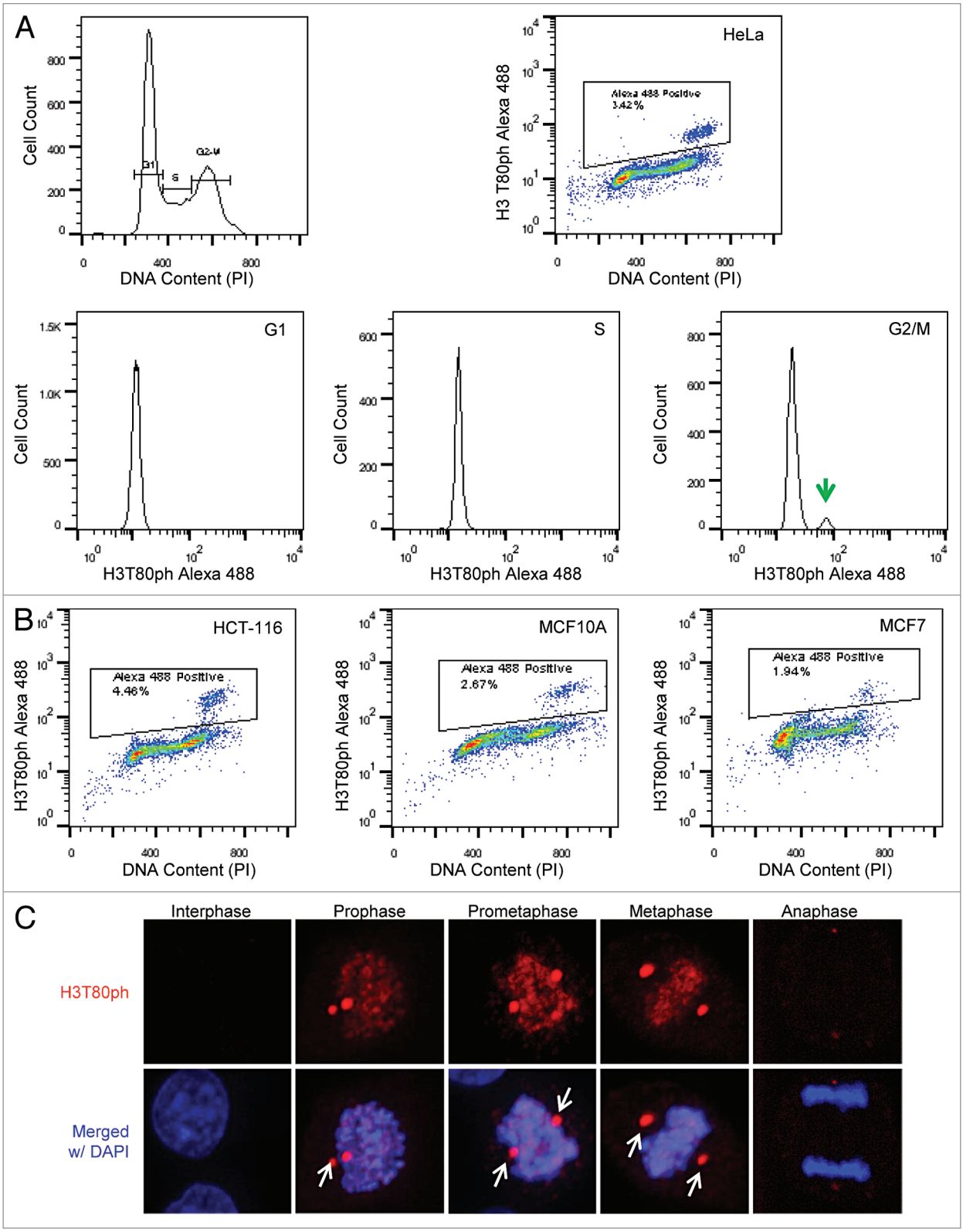

Figure 3. Histone H3T80 phosphorylation is enriched in mitosis. (**A**) Flow cytometry analysis of HeLa cells stained with anti-H3T80ph antibody using goat anti-rabbit Alexa Fluor® 488 as a secondary antibody and counter stained with propidium iodide (PI). Top left: The cell cycle profile using propidium iodide staining alone. Top right: Scatter plot of anti-H3T80ph staining vs. PI. Bottom: Cell number vs. anti-H3T80ph staining intensity during each phase of the cell cycle. The green arrow in the G_2 panel indicates the cells where anti-H3T80ph staining was enriched over background. (**B**) Flow cytometry analysis of HCT-116, MCF7, and MCF10A cell lines stained with anti-H3T80ph antibody using goat anti-rabbit Alexa Fluor® 488 as a secondary antibody and counter stained with PI. (**C**) Immunofluorescence analysis of methanol fixed HeLa cells using histone H3T80ph antibody. Arrows indicate centrosomes.

separation of localization underscores a potential separation of function for the H3S10ph and H3T80ph mitotic markers.

Mutations in H3T80 result in mitotic phenotypes

Because H3T80ph localizes to chromatin in mitosis, we asked whether loss of the phospho-regulation of histone H3 at this site might interfere with mitotic events. To do this, we transiently transfected, exogenous V5-His tagged wild-type and mutant histone H3T80 constructs into HeLa cells. The H3T80 mutations were designed to be either non-phosphorylatable (T80A) or to mimic constitutive phosphorylation (T80E). After verifying that the WT and mutant tagged proteins were associated with chromatin (**Fig. 5A, B, and D**), asynchronous cells were examined and categorized based on 3 parameters: (1) the phase of mitosis; (2) whether unaligned chromatin was present at metaphase; and (3) whether chromatin bridges were present in anaphase/telophase. These analyses showed that while there was no change in the percentage of the H3T80A mutants in any of the mitotic phases relative to WT, the H3T80E mutants displayed a small but significant increase in the number of cells in prophase, defined here based on the presence of a circular or near circular nucleus with condensing chromatin (**Fig. 5A**). Conversely, at anaphase, the H3T80A mutation, but not the H3T80E mutation, resulted in a significant increase in the number of cells with anaphase/telophase bridges, which have been associated previously with improper chromatin compaction[29,30] (**Fig. 5B**). No statistically significant defects in chromosome alignment at metaphase were detected for any of the H3 constructs (**Fig. 5B**). The transiently transfected histones were expressed to similar levels as each other, and they represented < 8% of the endogenous H3 level (**Fig. 5C**), making the observed mitotic phenotypes much more striking and highlighting the possible importance of H3T80ph for mitosis. In addition to these transient expression experiments, we also generated cell lines stably expressing wild-type H3 and H3T80E; however, H3T80A expression was not tolerated (data not shown), consistent with what might be expected due to more cells experiencing the mitotic defects described above.

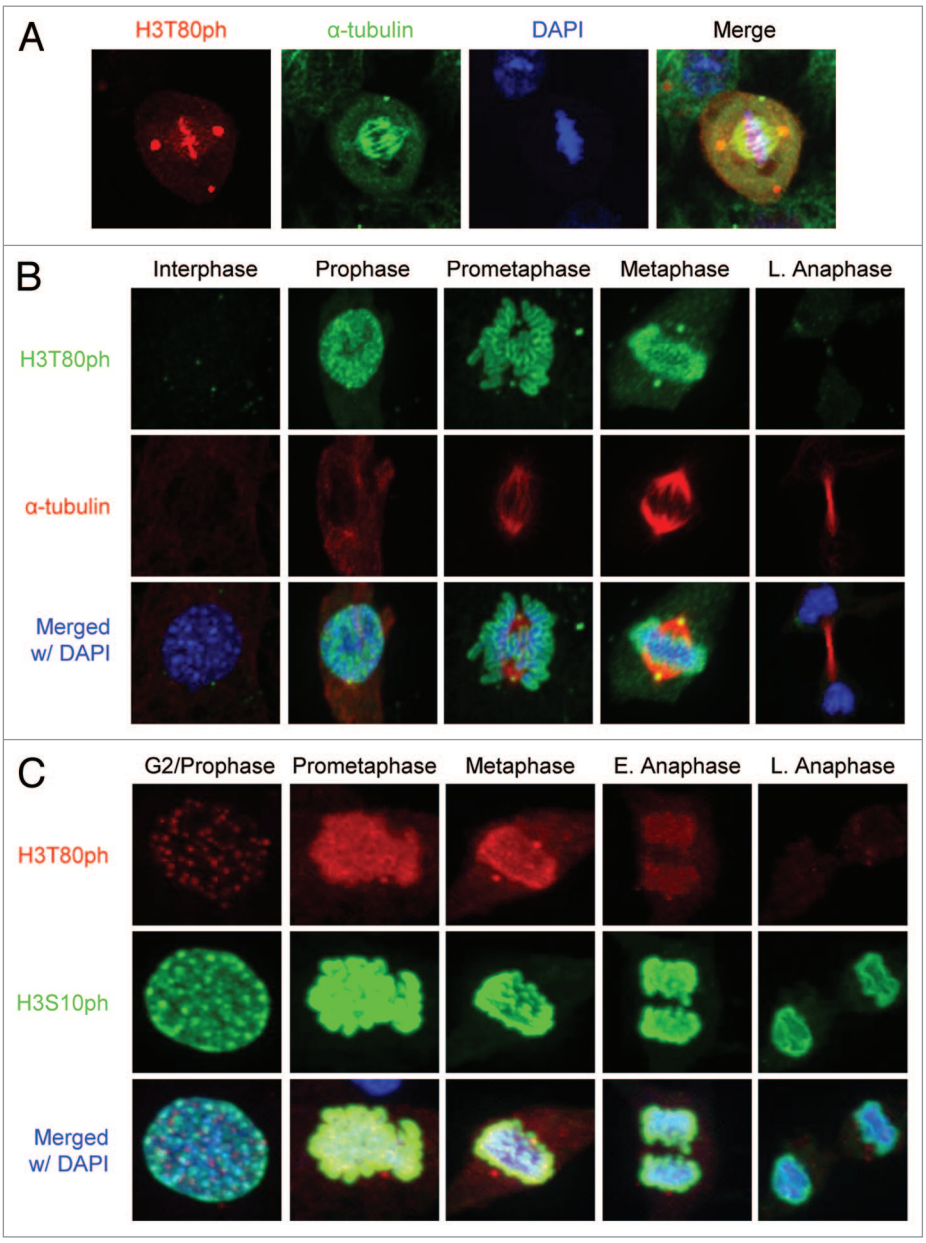

Figure 4. Histone H3T80 phosphorylation is conserved across metazoans. (**A**) Immunofluorescence analysis of *Drosophila* S2 cells using anti-H3T80ph antibody. Anti-α-tubulin staining was used to determine mitotic phase and to mark spindles. (**B**) Top: Immunofluorescence analysis of mouse MM3MG cells using anti-H3T80ph antibody. Middle: Anti-H3T80ph staining was compared with anti-α-tubulin staining. Bottom: Anti-H3T80ph and anti-α-tubulin staining merged with DAPI. (**C**) Top: Immunofluorescence analysis of mouse MM3MG cells using anti-H3T80ph antibody. Middle: Anti-H3T80ph staining was compared with anti-H3S10ph staining. Bottom: Anti-H3T80ph and anti-H3S10ph staining merged with DAPI.

H3T80ph preferentially binds to histone H2A and H4

To gain more insight into the molecular function of H3T80ph we used SILAC (stable isotope labeling by amino acids in cell culture) coupled mass spectrometry to identify potential binding partners for H3T80ph and H3T80 (**Fig. 6A**). The analysis uncovered 25 proteins that preferentially bound the H3T80ph peptide (**Tables S1 and S2**), including histones H2A and H4 (**Fig. 6B and C**). For the unmodified peptide, several kinases were enriched binding to H3T80 (**Table S3**), but they were either cytoplasmic or were discounted as the H3T80 kinase by inhibitor experiments (**Table S4**).

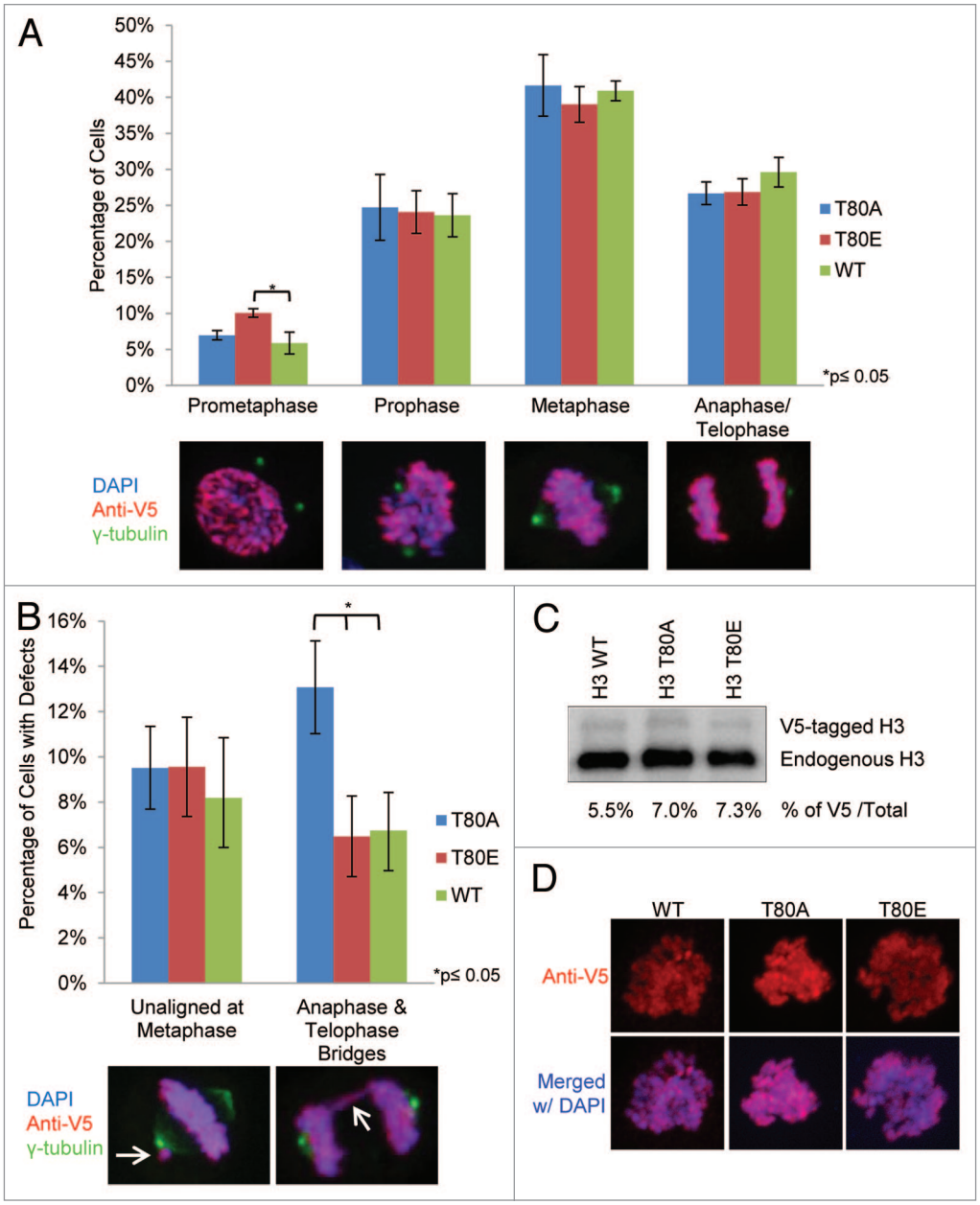

Figure 5. Expression of histone H3T80 mutants results in mitotic phenotypes. HeLa cells transiently expressing either wild type, T80A (unmodifiable), or T80E (phosphomimic) H3.1-V5/6xHis evaluated 48 h post transfection. (**A**) Cells were fixed and immunofluorescence was performed to detect V5 tagged H3.1 (red) and gamma tubulin (green). A representative cell is shown. Mitotic cells (300–500) were counted in each experiment and were classified based on their mitotic stage. Data shown is the average of 4 independent experiments. (**B**) The percentage of metaphase cells and anaphase/telophase cells from (**A**) with mitotic defects. A representative cell is shown with an arrow indicating the corresponding mitotic defect. (**C**) Representative western analysis of transfected cells using an N-term H3 antibody. The percentage of H3.1-V5/6xHis relative to the amount of total H3 is shown. (**D**) Immunofluorescence analysis of HeLa cells in prometaphase transiently expressing wild type, T80A, or T80E H3.1-V5/6xHis.

Therefore, a KinaseFinder (ProQinase) screen was performed in which 190 serine/threonine kinases were evaluated by in vitro kinase assays for their ability to phosphorylate an H3T80 peptide (**Fig S1**). An arbitrary threshold of 1500 cpm was set, and kinases that met this threshold or were near it and had known chromatin associations were subsequently tested by looking for a reduction or loss of H3T80ph immunofluorescence signal in HeLa cells grown in the presence of specific kinase inhibitors and/or shRNAs (**Table S4**). None of the tested kinases affected the levels of H3T80ph in vivo. Notably, VRK1, a known H3T3 and H3S10 kinase, showed some ability to phosphorylate H3T80 in the kinase screen, but further evaluation in cells has not been possible, because H3T80ph is only seen during mitosis and loss of VRK1 leads to G_1 arrest.[31] However, VRK1 is unlikely to phosphorylate H3T80, as Kang and colleagues showed via in vitro kinase assays that H3T3 and H3S10 are the only H3 sites phosphorylated by VRK1.[32] As such, the phosphorylation of H3T80 does not appear to be mediated by the kinases that phosphorylate

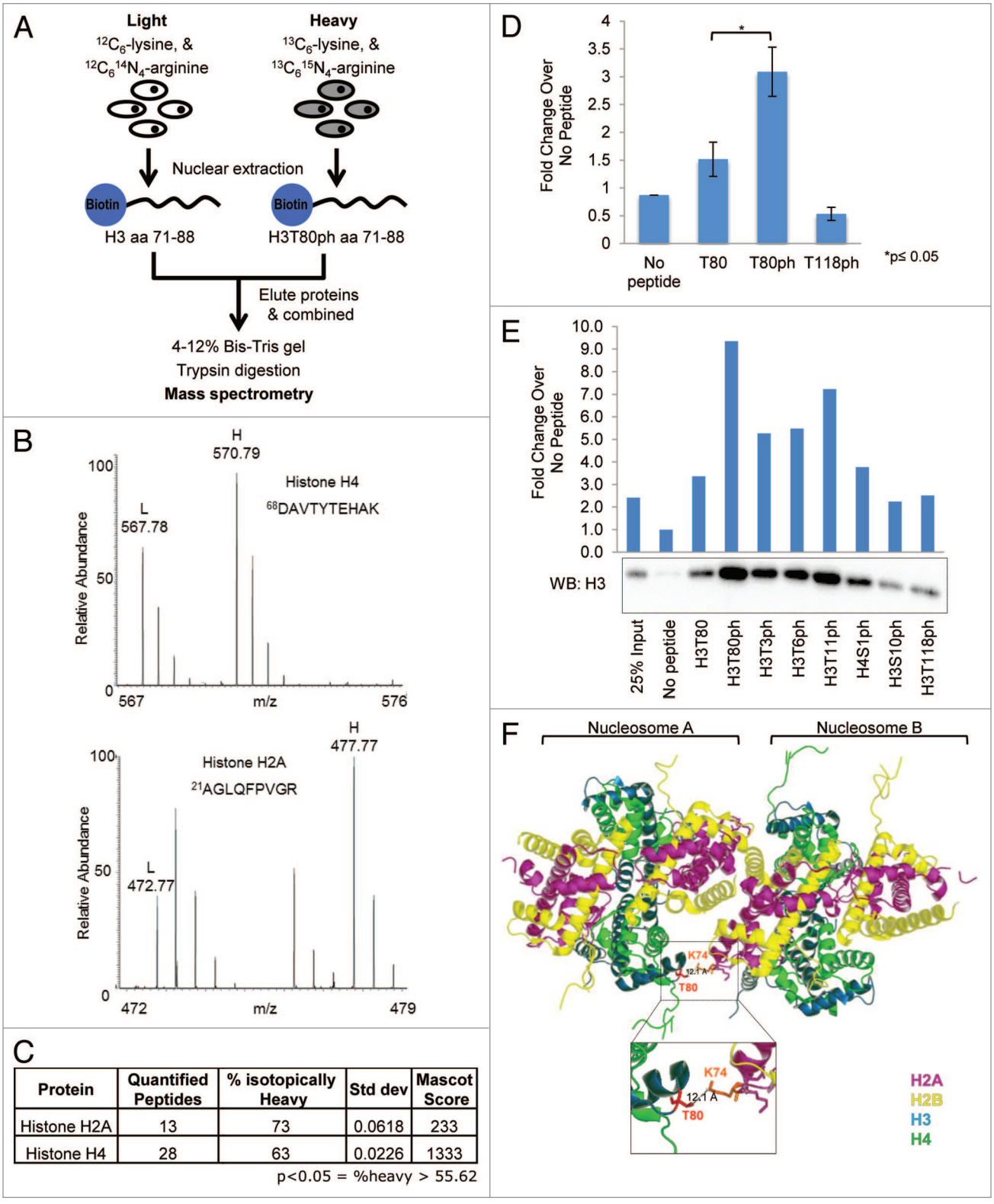

Figure 6. In vitro and structural data suggest that H3T80ph may promote nucleosome-nucleosome interactions. (**A**) Schematic illustrating SILAC approach to identify H3T80ph interacting proteins. (**B**) Representative high-resolution mass spectra from histone H2A (top) and histone H4 (bottom) peptides identified as specifically interacting with an H3T80ph peptide. (**C**) Quantification of the association of H2A and H4 with the H3T80ph peptide. (**D**) In vitro binding assay using recombinant histone octamers and the indicated peptides. (**E**) In vitro binding assay using recombinant histone octamers and the indicated peptides. Histogram is the average of 2 experiments. Representative western analysis of bound histone octamers using anti-histone H3. Histogram shows fold change over no peptide. (**F**) Two histone octamers from the tetranucleosome structure as solved by Schalch et al.[34] H3T80 is highlighted in red and H2AK74 is highlighted in orange.

the other H3 residues, and the H3T80 kinase currently remains unknown.

To independently verify that H3T80ph peptides can bind specifically to H2A and H4, we compared the ability of the H3T80ph peptide to bind histone octamers in in vitro binding assays. We consistently found that the H3T80ph peptide bound to the histone octamer 2–3-fold better than the unmodified H3T80 peptide and consistently better than the other phospho-histone H3 peptides, suggesting that the interaction cannot be attributed to H3 or phosphorylation alone (**Fig. 6D and E**). Given that the H3T80 side chain protrudes from the nucleosome surface, it is unlikely to promote intra-nucleosomal interactions, but rather inter-nucleosomal interactions, such as with the adjacent nucleosome. We propose that H3T80ph on one nucleosome interacts with H2A and H4 on the adjacent nucleosome to promote chromatin compaction during mitosis (**Fig. 6F** and discussed below).

Discussion

In this work, we provide the first characterization of a new histone modification, H3T80ph. We show that H3T80ph is a mitotic histone modification in human, mouse, and *Drosophila* cells. Mutation of H3T80 to mimic or prevent phosphorylation leads to mitotic delay and elevated levels of chromatin bridges, respectively, indicating that H3T80ph promotes normal events in mitosis. Protein–protein interaction analyses indicate that H3T80ph binds to histones, and given that this modification protrudes from the nucleosome surface, we propose that it mediates interactions with the adjacent nucleosomes to promote chromatin compaction during mitosis.

In addition to being spread throughout the chromatin during prophase-metaphase, H3T80ph is also seen at or near the centrosome at approximately the same cell cycle stages. It has been previously established that the proteasome can associate with centrosomes,[33] and we have evidence that excess free histone H3 is transported to the centrosomes for degradation specifically during mitosis (CL Wike and JK Tyler, unpublished data). Here, we focused on the function of H3T80ph within the chromatin, which we believe is independent of its role at the centrosomes.

The identification of histones H4 and H2A binding preferentially to the phosphorylated H3T80 peptide (**Fig. 6B and C**), and the finding that H3T80 phosphorylation enhances the interaction with histone octamers (**Fig. 6D and E**) suggests the possibility that H3T80ph may promote interactions with other histones. Given that H3T80ph protrudes from the nucleosome surface, we examined the tetranucleosome structure[34] to explore a potential model by which H3T80ph may enhance interaction with the adjacent nucleosome. To make H3T80 more apparent in the tetranucleosome model, we removed 2 of the nucleosomes, as well as the DNA. This simplified rendering reveals that H3T80ph is located close to histone H2A lysine 74 (H2A K74) of the adjacent histone octamer (**Fig. 6F**). H2AK74 itself is flanked by asparagine (H2AN73) and lysine (H2AK75) residues. These 3 residues are present at the end of α helix 2 and the beginning of loop L2 of the H2A histone fold and possess the potential and appropriate charge to interact with H3T80ph. This putative interaction between H3T80ph and H2A could assist in stabilizing the interactions between adjacent nucleosomes, thus aiding chromatin compaction during mitosis. Specific H3T80ph interacting residues on H4 are less obvious from the tetranucleosome structure. However, the tetranuclesome structure[33] represents only one model of nucleosome stacking,[35] making it conceivable that histone H4 may interact with H3T80ph through any of its exposed basic or amide residues. Noteworthy, the timing of appearance and disappearance of H3T80ph during mitosis coincides perfectly with the onset of chromatin compaction and the loss of chromatin compaction, respectively, during mitosis. In the future, biophysical analyses will be required to validate our proposed model for the interaction between H3T80ph and H2A in promoting chromatin fiber compaction. However, there is precedent for a histone modification regulating chromatin compaction, provided by acetylation of H4K16. The unacetylated H4 tail binds to an acidic patch formed by H2A/H2B on the surface of the adjacent nucleosome promoting formation of the 30-nm fiber, while acetylation breaks this interaction preventing chromatin fiber condensation.[36]

Even though the transiently expressed mutant histone H3 constitutes less than 10% of the total H3 in cells, expression of H3T80A that cannot be phosphorylated results in a significant increase in the percentage of mitotic cells with chromatin bridges (**Fig. 5B**). Chromatin bridges can result from errors in a variety of processes, including incomplete replication, telomere fusion, and improper chromosome condensation.[29,30,37,38] However, H3T80ph was not enriched until after replication at prophase, and its localization was not restricted to telomeres, making it unlikely that the chromatin bridges due to H3T80A expression are due to incomplete replication or telomere fusion, and more likely that there is a fault in chromosome condensation. Mutational studies in *S. cerevisiae* imply that the H3T80 residue lacks an important functional role[39,40] in that organism, which is consistent with the fact that mitotic chromosomes in yeast condense by about 2-fold in contrast to metazoan chromosomes that condense 4–50-fold during mitosis.[41]

Expression of the phosphorylation mimic H3T80E resulted in an increase in the proportion of cells in prophase (**Fig. 5A**), which could be due to more rapid chromatin condensation upon initiation of mitosis. While we have not ruled out the possibility that there is a true prophase delay, we postulate that the increase in H3T80E cells in prophase is not due to a delay in mitotic progression, but instead reflects an increase in the kinetics of chromatin condensation, resulting in their identification as prophase cells earlier in mitosis, a phenomenon that is conceivable if we take into consideration the fact that mitotic chromosome condensation can occur independently of other mitotic processes, particularly spindle assembly, as observed when cells are treated with microtubule-destabilizing agents.[28]

The identity of the H3T80 kinase may substantially enhance our understanding of the function of H3T80ph. Consequently, we tested multiple mitotic and non-mitotic kinases by in vitro and in vivo methods (**Table S4**; **Fig. S1**) but did not find convincing support for any of them mediating phosphorylation of H3T80. It is notable that Haspin, an atypical protein kinase that bears

little resemblance to the vast majority of protein kinases, appears to exclusively phosphorylate H3T3,[42,43] and that DOT1L, the methyltransferase for H3K79, is unusual among histone methyltransferases, as it lacks the SET domain common to the majority of methyltransferases.[23,44] With this considered, it is conceivable that the kinase for the adjacent H3T80 residue is also unique, and thus not readily predictable.

In summary, our results demonstrate that H3T80ph is a mitotic event that, while unique in its nucleosomal surface location, is similar to other mitotic phosphorylations in the timing of its addition and eventual removal from the mitotic chromatin. We propose that the protrusion of H3T80ph from the nucleosomal surface allows it to directly facilitate inter-nucleosome interactions, providing a potential mechanism that underlies proper chromosome condensation during mitosis in metazoans.

Materials and Methods

Cell culture

HeLa and MCF7 cells were maintained in Dulbecco modified Eagle medium (DMEM) supplemented with 10% fetal bovine serum and 1% penicillin/streptomycin. MCF10A cells were maintained in DMEM/nutrient mixture F-12 supplemented with 5% horse serum, 1% penicillin/streptomycin, 10 mg/ml insulin, 1 mg/ml hydrocortisone, 25 μg/ml EGF, and 1 mg/ml cholera toxin. HCT-116 cells were maintained in McCoy 5a Medium with 10% fetal bovine serum and 1% penicillin/streptomycin. MM3MG-HO cells were maintained in Dulbecco modified Eagle medium supplemented with 10% fetal bovine serum, 1% penicillin/streptomycin, 200 mM L-glutamine, 1% non-essential amino acids, and 1 μg/ml puromycin. All mammalian cell lines were maintained in 5% CO_2 at 37 °C. DT40 cells, a chicken B-cell line, were maintained in RPMI 1640 medium supplemented with 10% fetal bovine serum, 1% chicken serum, 50 uM β-mercaptoethanol, and 1% penicillin/streptomycin in 5% CO_2 at 40 °C. *Drosophila* S2 cells were maintained in Schneider's medium supplemented with 10% fetal bovine serum at room temperature.

Western blots

Approximately 2 × 10^6 cells were lysed with 200 μl of Laemmli buffer (4% SDS, 20% Glycerol, and 120 mM Tris pH 6.8). Cells were subsequently vortexed for 30 s and then placed at 100 °C for 5 min. After briefly cooling, samples were vortexed for 30 s, sonicated for 10 s at 20% power, and vortexed again for 30 s. Samples were resolved by 15% SDS-page and transferred to nitrocellulose according to standard procedure. Following transfer blots were blocked in 5% non-fat milk (w/v) in 1× TBST for 1 h. Primary antibodies were used at room temperature for 1 h or overnight at 4 °C and secondary antibodies were used at room temperature for 1 h. Alpha viewer was used to analyze and quantitate bands (Proteinsimple, http://www.proteinsimple.com/software_alphaview.html).

Dot blots

The indicated biotinylated peptides were serially diluted to the indicated concentrations and dotted out onto activated PVDF membrane. The membrane was allowed to absorb the peptides and then amido black staining was used to verify the presence of the peptides. The membranes were washed in PBS and then blocked in 3% BSA/1× PBS. Primary antibodies were used at room temperature for 1 h or overnight at 4 °C and secondary antibodies were used at room temperature for 1 h.

Immunofluorescence based peptide competition

Four μg of the indicated biotinylated peptides were incubated with 400 μl of the H3T80ph antibody for 45 min at room temperature (RT). Samples were centrifuged for 15 min at 4 °C at 13 k rpm. 300 μl of each supernatant was used for immunofluorescence.

Plasmids

Site directed mutagenesis was performed on the pcDNAV5/6xHis wild-type H3.1 plasmid using QuickChange Site-Directed Mutagenesis Kit (Agilent Technologies, http://www.genomics.agilent.com/en/Site-Directed-Mutagenesis/QuikChange/?cid=AG-PT-175&tabId=AG-PR-1160). The pcDNAV5/6xHis H3.1 T80E plasmid was generated using the following primers:

Forward: 5′-GAAATAGCTC AGGACTTCAA GGAGGACCTG CGCTTCCAGA GTTCC-3′

Reverse: 5′-GGAACTCTGG AAGCGCAGGT CCTCCTTGAA GTCCTGAGCT ATTTC-3′

Antibodies and peptides

Rabbit monoclonal H3T80ph antibodies were made by Epitomics and were maintained as hybridoma cell lines according to their instructions. The H3T80ph antibodies are used neat to 1:5 for immunofluorescence analyses. In addition to the H3T80ph antibodies the following primary antibodies were used: monoclonal H3K79me3T80ph (MC491) (Upstate), polyclonal H3K79me3T80ph (Millipore, http://www.millipore.com/catalogue/item/07-528), H3K79me2 (Abcam, http://www.abcam.com/histone-h3-methyl-di-k79-antibody-chip-grade-ab3594.html), H3S10ph (Abcam, http://www.abcam.com/histone-h3-phospho-s10-antibody-mabcam-14955-chip-grade-ab14955.html), C-terminal H3 (Abcam, http://www.abcam.com/histone-h3-antibody-chip-grade-ab1791.html), γ-tubulin (Abcam, http://www.abcam.com/gamma-tubulin-antibody-tu-30-ab27074.html), V5 (Millipore, http://www.millipore.com/catalogue/item/ab3792), phospho-p44/p42 MAPK (Cell Signaling, http://www.cellsignal.com/products/5726.html), mouse α-tubulin (Sigma-Aldrich, http://www.sigmaaldrich.com/catalog/product/sigma/t9026), and rat α-tubulin (http://www.abdserotec.com/yeast-tubulin-alpha-antibody-yol1-34-mca78g.html). The secondary antibodies used are as follows: Alexa Fluor® 488 goat anti-rabbit (Invitrogen, http://products.invitrogen.com/ivgn/product/A11034?ICID=search-product), Alexa Fluor® 594 goat anti-rabbit (Invitrogen, https://products.invitrogen.com/ivgn/product/A11037?ICID=search-a11037), Alexa Fluor® 488 goat anti-mouse (Invitrogen, https://products.invitrogen.com/ivgn/product/A11029?ICID=search-a11029), Alexa Fluor® 555 goat anti-rat (Cell Signaling, http://www.cellsignal.com/products/4417.html), HRP-conjugated anti-mouse, and HRP-conjugated anti-rabbit.

Biotinylated peptides were either purchased from Anaspec (https://www.anaspec.com/services/peptide.asp) or were a kind gift from Min Gyu Lee.

Immunoprecipitation

Eight × 10^6 HeLa cells were harvested and washed with 1× PBS. Cells were resuspended in 400 μl of cold histone extraction buffer (10 mM TRIS-HCl pH 7.5, 150 mM NaCl, 1.5 mM $MgCl_2$, 3% Glycerol, and 10 mM EDTA) by gently pipetting up and down 20 times while avoiding bubbles. Samples were overlaid onto 400 μl of cold histone glycerol solution (10 mM TRIS-HCl pH 7.5, 1.5 mM $MgCl_2$, and 25% glycerol) and then centrifuged 10 min at 4 °C at 5000 rpm. Supernatant was discarded and the pelleted nuclei were re-suspended in 100 μl of cold ChIP lysis buffer (1% SDS, 10 mM EDTA pH 8.0, and 50 mM NaCl). Samples were sonicated 3 times for 5 s at 30% power (output control 3, 100% duty cycle), while avoiding bubbles, with a 30 s rest between each sonication. Samples were diluted 1:10 in cold ChIP dilution buffer (1% Triton X-100, 2 mM EDTA, 150 mM NaCl, and 20 mM TRIS-HCl pH 8.1) and centrifuged at 4 °C at 13 k rpms for 5 min. The supernatant was retained and the proteins were quantified using Bio-Rad protein assay dye according to the microassay procedure (Bio-Rad, http://www.bio-rad.com/en-us/sku/500-0006-bio-rad-protein-assay-dye-reagent-concentratee). One hundred micrograms of total nuclear extract was further diluted to 300 μl using ChIP dilution buffer and precleared by adding 20 μl of 1× PBS washed Dynabeads® protein A and G (1:1) (Invitrogen, http://products.invitrogen.com/ivgn/product/10002D and https://products.invitrogen.com/ivgn/product/10009D) beads incubating for 1 h. 300 μl of the H3T80ph antibodies was added to the precleared extract and samples were incubated for 3 h. Twenty μl of Dynabeads® protein A and G (1:1) beads, which had been blocked in 10% BSA/1× PBS for 1 h, were added to the nuclear extract and incubate for 1 h. The supernatant was discarded, and the beads were washed 4 times with cold NETN (150 mM NaCl, 50 mM Tris pH7.5, 5 mM EDTA, and 0.5% NP40) for 10 min. All incubations and washes were performed at 4 °C on a nutator. Low adhesion tubes were used in all steps where beads were used (Bioexpress, http://www.bioexpress.com/divinity-cart/item/458600/GeneMate-1.7ml-Low-Adhesion-Thermo-Graduated-Tubes/1.html), and tubes were changed between washes. Thirty-five μl of 2× SDS buffer was added to the washed beads, which were then placed at 95 °C for 5 min and used for western blot.

Immunofluorescence

Cells were grown on poly-D-lysine-coated coverslips and harvested prior to reaching 80% confluency. Coverslips were washed in 1× PBS and fixed in 4% paraformaldehyde/1× PBS for 10 min at RT. Coverslips were washed in 1× PBS and then permeabilize with 1× PBS + 0.1% Triton X-100 at RT. Coverslips were then washed in 1× PBS and blocked in 3% BSA/1× PBS for 1 h. Primary antibodies were diluted into 3% BSA/1× PBS and incubated overnight at 4 °C. Coverslips were washed in 1× PBS prior to adding secondary antibodies. Coverslips were washed in 1× PBS and mounted onto glass slides with ProLong® Gold Antifade mounting reagent containing DAPI (Invitrogen, http://products.invitrogen.com/ivgn/product/P36931). Cells were imaged with a 3i Marianas Spinning Disk Confocal.

***Drosophila* immunofluorescence**

One × 10^6 *Drosophila* S2 cells were allowed to attach to 22 × 22 mm coverslips coated in 0.5 mg/ml Concanavalin A (Sigma) for 45 min in a sterile hood at RT. The coverslips were then washed in 1 X PBS before fixation in 10% EM grade paraformaldehyde for 10 min at RT. Cells were permeablized using 1× PBS + 0.1% Triton-X100 for 15 min at RT and then washed 3 times with 1× PBS. Cells were blocked in 5% normal donkey serum (NDS) diluted in 1× PBS + 0.1% Triton-X100 for 1 h at RT. Cells were then incubated overnight at 4 °C in H3T80ph (1:5) and rat α-tubulin (1:200) primary antibodies diluted in 5% NDS/0.1%Triton-X100/PBS. Cells were washed 3 times for 10 min each in 1× PBS + 0.1%Triton-X100 at RT on a rocking platform. Cells were incubated in Rb-Cy3 and Rt-Alexa488 (1:600 each; Jackson Immunoresearch) secondary antibodies diluted in 5% NDS/.1%Triton-X100/PBS for 1 h at RT and then washed 3 times 10 min each in 1× PBS+0.1%Triton-X100 at RT on a rocking platform. Coverslips were then mounted in ProLong® Gold Antifade mounting reagent containing DAPI, allowed to dry overnight at RT and imaged on an Olympus FV1000 confocal microscope.

Flow cytometry

Approximately 1 × 10^7 cells were washed in 1× PBS and then incubated for 10 min at 37 °C in 500 μl of 4% paraformaldehyde. Cells were permeablized by adding 4.5 mls of ice-cold 100% methanol and incubating on ice for 30 min. Cells were blocked in 3% BSA/1× PBS for 1 h and then placed in anti-H3T80ph (neat) at 4 °C overnight. After washing, Alexa488 anti-rabbit was used as a secondary. Cells were stained with propidium iodide and treated with RNase by incubating the cells for 30 min at 37 °C in a PI master mix (40 μg/ml propidium iodide and 100 μg/ml RNase in 1× PBS). Cells were analyzed using a Becton Dickinson FACS Calibur within 1 h of staining.

SILAC

Nuclear extracts were prepared from isotopically heavy ($^{13}C_6$-lysine, $^{13}C_6{}^{15}N_4$-arginine) and isotopically light Hela cells using the Active Motif Nuclear Extract Kit (Active Motif, http://www.activemotif.com/catalog/100/nuclear-extract-kit). The nuclear extract was diluted to 0.6 mg/mL in binding buffer (150 mM NaCl, 20 mM HEPES, pH 7.9, 1% NP40, 1 mM DTT, 1:100 protease inhibitor cocktail). Nuclear extracts from the light and heavy labeled cells were separately incubated for 2 h at 4 °C with 0.5 mg of streptavidin-coated Dynabeads (Life Technologies M280) coupled with either unmodified histone H3 peptide (with light nuclear extract) or histone H3T80ph peptide (with heavy nuclear extract). The beads were washed 5 times in 1 mL of binding buffer with an increased salt concentration (300 mM NaCL) and twice with low salt binding buffer (150 mM NaCl). Proteins were then eluted with Laemmli SDS-PAGE loading buffer, mixed 1:1 for light and heavy nuclear extract incubations, and resolved on a 4–12% Bis-Tris gel and visualized by Coomassie staining. The gel lane was sliced into 2-mm sections and subjected to in-gel trypsin digestion.[45-47] The peptides were identified by high-resolution mass spectrometry with a Thermo Velos Orbitrap mass spectrometer equipped with a Waters nanoACQUITY UPLC system. Proteins and PTM-containing peptides were identified and the percent heavy for each peptide was calculated as $I_H/(I_H+I_L)$ with MASCOT Distiller.[45] The average percent heavy of all peptides identified for each protein was calculated along with the

standard deviation. Once proteins were identified and the percent of isotopically heavy was calculated, a contaminant threshold was established based on 32 nonspecifically enriched ribosomal proteins as previously reported in references 45, 48, and 49, resulting in a nonspecifically associating baseline of 42 ± 0.14% isotopically heavy. Using 2 standard deviations from this baseline as the significance level, 25 proteins were found to specifically interact with H3T80ph (**Table S2**), while 137 proteins were determined to be non-specific associations (**Table S3**).

Peptide binding assay

Twenty microlitre of Streptavidin-coupled Dynabeads® (Invitrogen, http://products.invitrogen.com/ivgn/product/11205D) were washed in binding buffer (50 mM Tris pH7.5, 100 mM NaCl, 0.05% NP40). Beads were re-suspended in 195 μl of binding buffer. Five μl of 1 μg/μl biotinylated peptides were added to the beads and placed on a nutator overnight at 4 °C. Beads were washed 3 times in binding buffer and then split into 2 tubes per sample. The total volume of each tube was brought up to 190 μl. Ten microliters of 0.45 μg/μl recombinant histone octamers[50,51] were added and allowed to bind on a nutator for 2–3 h at 4 °C. Samples were washed 3 times in binding buffer and histones were eluted with 2× SDS loading buffer and analyzed by western blot.

Disclosure of Potential Conflicts of Interest

No potential conflicts of interest were disclosed.

Acknowledgments

We are extremely grateful to Noel Lowndes for the DT40 cells. pcDNAV5/6xHis wild-type H3.1 and H3.1T80A plasmids were a gift from Estela Medrano. We thank Varija Budhavarapu for recombinant histone octamers. We thank Estela Medrano for her guidance during the early stage of this project and Siddhartha Roy for help with structural models. This work was supported by GM grant GM64475 to JKT and CPRIT rising star, UT Texas Stars, and Senior Trust recruitment awards to JKT.

Supplemental Materials

Supplemental materials may be found here:
www.landesbioscience.com/journals/cc/article/27269

References

1. Luger K, Mäder AW, Richmond RK, Sargent DF, Richmond TJ. Crystal structure of the nucleosome core particle at 2.8 A resolution. Nature 1997; 389:251-60; PMID:9305837; http://dx.doi.org/10.1038/38444
2. Jenuwein T, Allis CD. Translating the histone code. Science 2001; 293:1074-80; PMID:11498575; http://dx.doi.org/10.1126/science.1063127
3. Tropberger P, Schneider R. Scratching the (lateral) surface of chromatin regulation by histone modifications. Nat Struct Mol Biol 2013; 20:657-61; PMID:23739170; http://dx.doi.org/10.1038/nsmb.2581
4. Polioudaki H, Markaki Y, Kourmouli N, Dialynas G, Theodoropoulos PA, Singh PB, Georgatos SD. Mitotic phosphorylation of histone H3 at threonine 3. FEBS Lett 2004; 560:39-44; PMID:14987995; http://dx.doi.org/10.1016/S0014-5793(04)00060-2
5. Hendzel MJ, Wei Y, Mancini MA, Van Hooser A, Ranalli T, Brinkley BR, Bazett-Jones DP, Allis CD. Mitosis-specific phosphorylation of histone H3 initiates primarily within pericentromeric heterochromatin during G2 and spreads in an ordered fashion coincident with mitotic chromosome condensation. Chromosoma 1997; 106:348-60; PMID:9362543; http://dx.doi.org/10.1007/s004120050256
6. Preuss U, Landsberg G, Scheidtmann KH. Novel mitosis-specific phosphorylation of histone H3 at Thr11 mediated by Dlk/ZIP kinase. Nucleic Acids Res 2003; 31:878-85; PMID:12560483; http://dx.doi.org/10.1093/nar/gkg176
7. Goto H, Tomono Y, Ajiro K, Kosako H, Fujita M, Sakurai M, Okawa K, Iwamatsu A, Okigaki T, Takahashi T, et al. Identification of a novel phosphorylation site on histone H3 coupled with mitotic chromosome condensation. J Biol Chem 1999; 274:25543-9; PMID:10464286; http://dx.doi.org/10.1074/jbc.274.36.25543
8. Hurd PJ, Bannister AJ, Halls K, Dawson MA, Vermeulen M, Olsen JV, Ismail H, Somers J, Mann M, Owen-Hughes T, et al. Phosphorylation of histone H3 Thr-45 is linked to apoptosis. J Biol Chem 2009; 284:16575-83; PMID:19363025; http://dx.doi.org/10.1074/jbc.M109.005421
9. Tweedie-Cullen RY, Brunner AM, Grossmann J, Mohanna S, Sichau D, Nanni P, Panse C, Mansuy IM. Identification of combinatorial patterns of post-translational modifications on individual histones in the mouse brain. PLoS One 2012; 7:e36980; PMID:22693562; http://dx.doi.org/10.1371/journal.pone.0036980
10. Tweedie-Cullen RY, Reck JM, Mansuy IM. Comprehensive mapping of post-translational modifications on synaptic, nuclear, and histone proteins in the adult mouse brain. J Proteome Res 2009; 8:4966-82; PMID:19737024; http://dx.doi.org/10.1021/pr9003739
11. Vermeulen M, Eberl HC, Matarese F, Marks H, Denissov S, Butter F, Lee KK, Olsen JV, Hyman AA, Stunnenberg HG, et al. Quantitative interaction proteomics and genome-wide profiling of epigenetic histone marks and their readers. Cell 2010; 142:967-80; PMID:20850016; http://dx.doi.org/10.1016/j.cell.2010.08.020
12. Huttlin EL, Jedrychowski MP, Elias JE, Goswami T, Rad R, Beausoleil SA, Villén J, Haas W, Sowa ME, Gygi SP. A tissue-specific atlas of mouse protein phosphorylation and expression. Cell 2010; 143:1174-89; PMID:21183079; http://dx.doi.org/10.1016/j.cell.2010.12.001
13. North JA, Javaid S, Ferdinand MB, Chatterjee N, Picking JW, Shoffner M, Nakkula RJ, Bartholomew B, Ottesen JJ, Fishel R, et al. Phosphorylation of histone H3(T118) alters nucleosome dynamics and remodeling. Nucleic Acids Res 2011; 39:6465-74; PMID:21576235; http://dx.doi.org/10.1093/nar/gkr304
14. Hsu JY, Sun ZW, Li X, Reuben M, Tatchell K, Bishop DK, Grushcow JM, Brame CJ, Caldwell JA, Hunt DF, et al. Mitotic phosphorylation of histone H3 is governed by Ipl1/aurora kinase and Glc7/PP1 phosphatase in budding yeast and nematodes. Cell 2000; 102:279-91; PMID:10975519; http://dx.doi.org/10.1016/S0092-8674(00)00034-9
15. Giet R, Glover DM. Drosophila aurora B kinase is required for histone H3 phosphorylation and condensin recruitment during chromosome condensation and to organize the central spindle during cytokinesis. J Cell Biol 2001; 152:669-82; PMID:11266459; http://dx.doi.org/10.1083/jcb.152.4.669
16. Adams RR, Maiato H, Earnshaw WC, Carmena M. Essential roles of Drosophila inner centromere protein (INCENP) and aurora B in histone H3 phosphorylation, metaphase chromosome alignment, kinetochore disjunction, and chromosome segregation. J Cell Biol 2001; 153:865-80; PMID:11352945; http://dx.doi.org/10.1083/jcb.153.4.865
17. Kelly AE, Ghenoiu C, Xue JZ, Zierhut C, Kimura H, Funabiki H. Survivin reads phosphorylated histone H3 threonine 3 to activate the mitotic kinase Aurora B. Science 2010; 330:235-9; PMID:20705815; http://dx.doi.org/10.1126/science.1189505
18. Hirota T, Lipp JJ, Toh BH, Peters JM. Histone H3 serine 10 phosphorylation by Aurora B causes HP1 dissociation from heterochromatin. Nature 2005; 438:1176-80; PMID:16222244; http://dx.doi.org/10.1038/nature04254
19. Fischle W, Tseng BS, Dormann HL, Ueberheide BM, Garcia BA, Shabanowitz J, Hunt DF, Funabiki H, Allis CD. Regulation of HP1-chromatin binding by histone H3 methylation and phosphorylation. Nature 2005; 438:1116-22; PMID:16222246; http://dx.doi.org/10.1038/nature04219
20. Wei Y, Yu L, Bowen J, Gorovsky MA, Allis CD. Phosphorylation of histone H3 is required for proper chromosome condensation and segregation. Cell 1999; 97:99-109; PMID:10199406; http://dx.doi.org/10.1016/S0092-8674(00)80718-7
21. MacCallum DE, Losada A, Kobayashi R, Hirano T. ISWI remodeling complexes in Xenopus egg extracts: identification as major chromosomal components that are regulated by INCENP-aurora B. Mol Biol Cell 2002; 13:25-39; PMID:11809820; http://dx.doi.org/10.1091/mbc.01-09-0441
22. de la Barre AE, Angelov D, Molla A, Dimitrov S. The N-terminus of histone H2B, but not that of histone H3 or its phosphorylation, is essential for chromosome condensation. EMBO J 2001; 20:6383-93; PMID:11707409; http://dx.doi.org/10.1093/emboj/20.22.6383
23. Feng Q, Wang H, Ng HH, Erdjument-Bromage H, Tempst P, Struhl K, Zhang Y. Methylation of H3-lysine 79 is mediated by a new family of HMTases without a SET domain. Curr Biol 2002; 12:1052-8; PMID:12123582; http://dx.doi.org/10.1016/S0960-9822(02)00901-6

24. van Leeuwen F, Gafken PR, Gottschling DE. Dot1p modulates silencing in yeast by methylation of the nucleosome core. Cell 2002; 109:745-56; PMID:12086673; http://dx.doi.org/10.1016/S0092-8674(02)00759-6
25. Shanower GA, Muller M, Blanton JL, Honti V, Gyurkovics H, Schedl P. Characterization of the grappa gene, the Drosophila histone H3 lysine 79 methyltransferase. Genetics 2005; 169:173-84; PMID:15371351; http://dx.doi.org/10.1534/genetics.104.033191
26. Martinez DR, Richards HW, Lin Q, Torres-Cabala CA, Prieto VG, Curry JL, Medrano EE. H3K79me3T80ph is a Novel Histone Dual Modification and a Mitotic Indicator in Melanoma. J Skin Cancer 2012; 2012:823534; PMID:23227340; http://dx.doi.org/10.1155/2012/823534
27. FitzGerald J, Moureau S, Drogaris P, O'Connell E, Abshiru N, Verreault A, Thibault P, Grenon M, Lowndes NF. Regulation of the DNA damage response and gene expression by the Dot1L histone methyltransferase and the 53Bp1 tumour suppressor. PLoS One 2011; 6:e14714; PMID:21383990; http://dx.doi.org/10.1371/journal.pone.0014714
28. Sluder G. Role of spindle microtubules in the control of cell cycle timing. J Cell Biol 1979; 80:674-91; PMID:572367; http://dx.doi.org/10.1083/jcb.80.3.674
29. Green LC, Kalitsis P, Chang TM, Cipetic M, Kim JH, Marshall O, Turnbull L, Whitchurch CB, Vagnarelli P, Samejima K, et al. Contrasting roles of condensin I and condensin II in mitotic chromosome formation. J Cell Sci 2012; 125:1591-604; PMID:22344259; http://dx.doi.org/10.1242/jcs.097790
30. Gerlich D, Hirota T, Koch B, Peters JM, Ellenberg J. Condensin I stabilizes chromosomes mechanically through a dynamic interaction in live cells. Curr Biol 2006; 16:333-44; PMID:16488867; http://dx.doi.org/10.1016/j.cub.2005.12.040
31. Kim IJ, Quigley D, To MD, Pham P, Lin K, Jo B, Jen KY, Raz D, Kim J, Mao JH, et al. Rewiring of human lung cell lineage and mitotic networks in lung adenocarcinomas. Nat Commun 2013; 4:1701; PMID:23591868; http://dx.doi.org/10.1038/ncomms2660
32. Kang TH, Park DY, Choi YH, Kim KJ, Yoon HS, Kim KT. Mitotic histone H3 phosphorylation by vaccinia-related kinase 1 in mammalian cells. Mol Cell Biol 2007; 27:8533-46; PMID:17938195; http://dx.doi.org/10.1128/MCB.00018-07
33. Wigley WC, Fabunmi RP, Lee MG, Marino CR, Muallem S, DeMartino GN, Thomas PJ. Dynamic association of proteasomal machinery with the centrosome. J Cell Biol 1999; 145:481-90; PMID:10225950; http://dx.doi.org/10.1083/jcb.145.3.481
34. Schalch T, Duda S, Sargent DF, Richmond TJ. X-ray structure of a tetranucleosome and its implications for the chromatin fibre. Nature 2005; 436:138-41; PMID:16001076; http://dx.doi.org/10.1038/nature03686
35. Nishino Y, Eltsov M, Joti Y, Ito K, Takata H, Takahashi Y, Hihara S, Frangakis AS, Imamoto N, Ishikawa T, et al. Human mitotic chromosomes consist predominantly of irregularly folded nucleosome fibres without a 30-nm chromatin structure. EMBO J 2012; 31:1644-53; PMID:22343941; http://dx.doi.org/10.1038/emboj.2012.35
36. Shogren-Knaak M, Ishii H, Sun JM, Pazin MJ, Davie JR, Peterson CL. Histone H4-K16 acetylation controls chromatin structure and protein interactions. Science 2006; 311:844-7; PMID:16469925; http://dx.doi.org/10.1126/science.1124000
37. van Steensel B, Smogorzewska A, de Lange T. TRF2 protects human telomeres from end-to-end fusions. Cell 1998; 92:401-13; PMID:9476899; http://dx.doi.org/10.1016/S0092-8674(00)80932-0
38. Chan KL, Palmai-Pallag T, Ying S, Hickson ID. Replication stress induces sister-chromatid bridging at fragile site loci in mitosis. Nat Cell Biol 2009; 11:753-60; PMID:19465922; http://dx.doi.org/10.1038/ncb1882
39. Dai J, Hyland EM, Yuan DS, Huang H, Bader JS, Boeke JD. Probing nucleosome function: a highly versatile library of synthetic histone H3 and H4 mutants. Cell 2008; 134:1066-78; PMID:18805098; http://dx.doi.org/10.1016/j.cell.2008.07.019
40. Nakanishi S, Sanderson BW, Delventhal KM, Bradford WD, Staehling-Hampton K, Shilatifard A. A comprehensive library of histone mutants identifies nucleosomal residues required for H3K4 methylation. Nat Struct Mol Biol 2008; 15:881-8; PMID:18622391; http://dx.doi.org/10.1038/nsmb.1454
41. Belmont AS. Mitotic chromosome structure and condensation. Curr Opin Cell Biol 2006; 18:632-8; PMID:17046228; http://dx.doi.org/10.1016/j.ceb.2006.09.007
42. Higgins JM. Structure, function and evolution of haspin and haspin-related proteins, a distinctive group of eukaryotic protein kinases. Cell Mol Life Sci 2003; 60:446-62; PMID:12737306; http://dx.doi.org/10.1007/s000180300038
43. Dai J, Sultan S, Taylor SS, Higgins JM. The kinase haspin is required for mitotic histone H3 Thr 3 phosphorylation and normal metaphase chromosome alignment. Genes Dev 2005; 19:472-88; PMID:15681610; http://dx.doi.org/10.1101/gad.1267105
44. Min J, Feng Q, Li Z, Zhang Y, Xu RM. Structure of the catalytic domain of human DOT1L, a non-SET domain nucleosomal histone methyltransferase. Cell 2003; 112:711-23; PMID:12628190; http://dx.doi.org/10.1016/S0092-8674(03)00114-4
45. Smart SK, Mackintosh SG, Edmondson RD, Taverna SD, Tackett AJ. Mapping the local protein interactome of the NuA3 histone acetyltransferase. Protein Sci 2009; 18:1987-97; PMID:19621382; http://dx.doi.org/10.1002/pro.212
46. Tackett AJ, DeGrasse JA, Sekedat MD, Oeffinger M, Rout MP, Chait BT. I-DIRT, a general method for distinguishing between specific and nonspecific protein interactions. J Proteome Res 2005; 4:1752-6; PMID:16212429; http://dx.doi.org/10.1021/pr050225e
47. Tackett AJ, Dilworth DJ, Davey MJ, O'Donnell M, Aitchison JD, Rout MP, Chait BT. Proteomic and genomic characterization of chromatin complexes at a boundary. J Cell Biol 2005; 169:35-47; PMID:15824130; http://dx.doi.org/10.1083/jcb.200502104
48. Byrum SD, Raman A, Taverna SD, Tackett AJ. ChAP-MS: a method for identification of proteins and histone posttranslational modifications at a single genomic locus. Cell Rep 2012; 2:198-205; PMID:22840409; http://dx.doi.org/10.1016/j.celrep.2012.06.019
49. Byrum SD, Taverna SD, Tackett AJ. Quantitative analysis of histone exchange for transcriptionally active chromatin. J Clin Bioinforma 2011; 1:17; PMID:21884633; http://dx.doi.org/10.1186/2043-9113-1-17
50. Luger K, Rechsteiner TJ, Richmond TJ. Preparation of nucleosome core particle from recombinant histones. Methods Enzymol 1999; 304:3-19; PMID:10372352; http://dx.doi.org/10.1016/S0076-6879(99)04003-3
51. Dyer PN, Edayathumangalam RS, White CL, Bao Y, Chakravarthy S, Muthurajan UM, Luger K. Reconstitution of nucleosome core particles from recombinant histones and DNA. Methods Enzymol 2004; 375:23-44; PMID:14870657; http://dx.doi.org/10.1016/S0076-6879(03)75002-2